CHAPTER IV
ROLE OF PLA-*b*-PBS ON COMPATIBILITY OF POLY(LACTIC ACID)/POLY(BUTYLENE SUCCINATE) MULTI-LAYERED FILMS

4.1 Abstract

Poly(lactic acid-*b*-butylene succinate) (PLA-*b*-PBS) copolymer as a compatibilizer for poly(lactic acid) and poly(buthylene succinate) in multi-layered film form is proposed. The use of conjugating agent in chloroform enables us to easily prepare block copolymer, PLA-*b*-PBS. By simple blending PLA-*b*-PBS in PBS, and applying this mixture in co-extrusion process to prepare the three layers of PLA/PBS containing PLA-*b*-PBS/PLA, the film obtained shows the compatibility, in other words, interfacial adhesion, as evidenced from the scanning electron micrographs. An increase of PLA-*b*-PBS copolymer content in PBS layer also leads to an increase in the oxygen barrier, and mechanical properties, especially an elongation at break.

Keyword: poly(lactic acid), poly(butylene succinate), multi-layered film, PLA-*b*-PBS copolymer, compatibilizer

4.2 Introduction

Multi-layered film is a potential technique to combine two or more polymers films together. In general, film co-extrusion to produce multi-layered films has its own advantages in terms of one-step, continuous, and versatile processes.[1] The product examples are usually packaging films, for example syringe packaging, cheese packaging, and rice packaging.[2] At present conventional multi-layered films are made from petroleum-based polymers such as polyethylene/polyamide, polyehtylene/poly(ethylene vinyl alcohol), etc.[3]

Nowadays, biodegradable polymers play an important role in terms of environmetal friendly. However, the main limitation of biodegradable polymers is quite expensive. Based on this viewpoint, value-added product produced from biodegradable multi-layered film is proposed.

The potential biodegradable polymers are poly(lactic acid) (PLA) and poly(butylene succinate) (PBS) regarding to the high strength and transparency of PLA and high toughness of PBS. Although the studies on the multi-layered film of PLA and PBS have been reported[4], the point about phase separation of each layer including oxygen permeability was not well clarified. It should be pointed that the combination of different polymer layers possibly brings in the phase separation and this leads to the poor mechanical properties.

In the past, inorganic compounds[5], crosslinkers[6], and copolymers[7] were reported. To our point of view, the solution of phase separation in multi-layered film might be possible if the compatibilizer is a copolymer that contains all polymer species appeared in the multi-layered film.

The present work focuses on the three-layered film of PLA/PBS/PLA, and demonstrates how PLA-*b*-PBS copolymer can play the role as compatibilizer to enhace the interfacial interaction between PLA and PBS. Here, a simple conjugating reaction using dicyclohexylcarbodiimide to obtain PLA-*b*-PBS is proposed. The studies also clarify how the addition of PLA-*b*-PBS in PBS results in enhancing the compatibility as well as improving the mechanical properties. Moreover, oxygen permeability of the PLA/PBS/PLA multi-layered films also studies.

4.3 Experimental Section

4.3.1 Materials

The commercial PLA (trade name 2003D) was purchased from NatureWorks LLC, USA (M_w = 287,900, M_n = 163,500). The commercial PBS (trade name GS-Pla) was bought from the Mitsubishi Chemicals Co., Ltd, Japan (M_w = 47,000, M_n = 37,000). L-lactic acid (L-LA) (with 88 wt% aqueous solution) was a gift from PURAC, Thailand. Analytical-grade 1,4-butanediol (with 99% purity) and tin(II)-2-ethylhexanoate ($SnOCt_2$) (with 95% purity) were purchased from Sigma-Aldrich, USA. Analytical-grade succinic acid (with 99% purity) was bought from Ajax, Australia. *N-N'*-dicyclohexylcarbodiimide (DCC) (with 99% purity) was purchased from Fluka, Germany. 4-Dimethylaminopyridine (DMAP) (with 99% purity) was bought from MERCK, Germany.

4.3.2 Instruments

4.3.2.1 Structural Characterization

Structural characterization was carried out by an Ultrashield 500 Plus Bruker spectrometer (500 MHz) at room temperature. The samples were dissolved in $CDCl_3$. The chemical shifts were calibrated by using the residual resonance of the solvent peak (7.26 ppm). An ALPHA Tensor series Bruker fourier-transform infrared spectrometer with 32 scans at a resolution of 4 cm^{-1} was used to investigate architecture polymer. The spectra were acquired and manipulated with the use of OPUS software. Molecular weight (MW) was measured by a Shimadzu Class-VP gel permeation chromatograph (GPC) equipped with a Polymer Lab PLgel 5 μm MIXED-D column using a reflective index detector. Chloroform (HPLC grade) was used as an eluent at a flow rate of 1.0 mL min^{-1}. Polystyrene standards were used for a calibration curve. The system was performed at 40 °C and the injection volume was 20 μm. Before measurement, the solution was filtered by using a 0.45 μm syringe filter.

4.3.2.2 Thermal Analysis

Glass transition temperature (T_g), melting temperature (T_m), and percent of crystallinity (X_c) of the multi-layered films were measured by a DSC 200 F3 Maia NETZCH differential scanning calorimetry (DSC) under nitrogen

atmosphere. The multi-layered films (~5 mg) were heated at 5 °C min^{-1}. The temperature ranged between -50 and +200 °C. The crystallinity (X_c) of the multi-layered films was calculated by the equation below:[8]

$$X_c = \frac{\Delta H_m - \Delta H_c}{\Delta H_m^0 \times f} \times 100\% \quad (1)$$

where ΔH_m and ΔH_c are the enthalpy of melting and crystallization determined by integrating the areas (J/g) under the peaks. ΔH_m^o is the reference value of melting enthalpy which represents the perfect crystalline PLA homopolymer (93.01 J/g).[9] All of the data was determined through first heating scan.

4.3.2.3 Mechanical Testing

Mechanical properties of multi-layered films were measured on a LRX LLOYD universal testing machine with a 500 N load cell. The testing was followed the ASTM D638M-91a. The five specimens were tested on each test.

4.3.2.4 Morphology Analysis

Morphology of the fracture surface of multi-layered films was investigated by a TM3000 Hitachi scanning electron microscope (SEM). The specimens were coated with a thin layer of platinum. The accelerating voltage of SEM system was 15 kV.

4.3.2.5 Barrier Study

Oxygen permeability was evaluated by an Ox-Tran 2/21 MOCON oxygen analyzer with an oxygen flow rate 20 cm^3/min at 23 °C at 0% RH. The testing was carried out according to ASTM D3985-81.

4.3.2.6 X-ray Diffraction

A Rigaku X-ray diffractometer was applied to determine crystalline pattern of the samples. X-ray diffraction (XRD) experiments were run using Cu Kα radiation and operated at 40 kV/30 mA.

4.3.3 Methodology

4.3.3.1 PLA Prepolymer Preparation

PLA prepolymer was carried out through polycondensation of L-LA (25.59 mL, 1 mol). The solution was added into a three-necked round-

bottom flask and magnetically stirred in an oil bath at 100 °C for 2 h under vacuum. $SnOCt_2$ (0.1 mol% of L-LA) was added into the reaction and the reaction was carried out at 150 °C for 24 h to obtain a viscous product. The product was dissolved in chloroform and was precipitated in cold methanol before washing with methanol several times. The precipitates were collected by filtrating and drying in vacuum. The characterization of PLA prepolymer was performed with ^{1}H NMR (500 MHz, $CDCl_3$): 1.59-1.61 (3H, d, -O-CH(C**H**$_3$)-), 4.36-4.40 (1H, d, HO-C**H**-(C=O)-), and 5.16-5.20 (1H, q, -O-C**H**(CH_3)-).

4.3.3.2 PBS Prepolymer Preparation

PBS prepolymer was synthesized through the poly-condensation between 1,4-butanediol (9.75 mL, 0.11 mol) and succinic acid (11.81 g, 0.1 mol). The reactants in a round-bottom flask was heated and stirred at 190 °C for 6 h under vacuum. The obtained product was collected in the same way as PLA prepolymer. Structure of PBS was characterized with ^{1}H NMR (500 MHz, $CDCl_3$): 1.72 (4H, s, -O-CH_2-C**H**$_2$-), 2.63 (4H, s, -(C=O)-C**H**$_2$-), 3.49 (2H, s, HO-C**H**$_2$-CH_2-), and 4.13 (4H, s, -O-C**H**$_2$-CH_2-).

4.3.3.3 Synthesis of PLA-b-PBS Copolymer

The PLA prepolymer (MW =1200-2200) (12 g, 6 mmol) and DMAP (73.3 mg, 10 mol%) were mixed, dissolved in CH_2Cl_2 (120 mL), and stirred for 10 min at room temperature. DCC solution (1.24 g, 6 mmol, 13 mL CH_2Cl_2) was charged in the reaction for 10 min. The PBS prepolymer (MW = 2000-3000) (21.5 g, 10 mmol) was dissolved in 215 mL of CH_2Cl_2 and added into the reaction. The mixture solution was continued for 36 h at room temperature. The precipitates in the reaction were filtered and then residual solution was heated to evaporate excess solvent. The product obtained was precipitated, before washing, and drying to obtain PLA-*b*-PBS.

4.3.3.4 PLA/PBS/PLA Multi-layered Films Procedure

PLA and PBS were co-extruded by using a LBE12.5-30 Labtech Engineering multi-layred film blowing line to obtain three-layered films so that PLA was on both outer layers and PBS was in the middle layer. The temperature and screw speed settings were in range of 140-180 °C and 40-50 rpm, respectively. For multi-layered films which contained PLA-*b*-PBS, the PBS resin was priority

mixed with PLA-*b*-PBS in various ratios, i.e. 0.5, 1, 3, and 5 phr, before co-extruding with PLA. Six different multi-layered films were prepared as quoted in Table 4.1

Table 4.1 Structure of multi-layered films and contents of PLA-*b*-PBS in PBS phase

Multi-layered film	Content of PLA-*b*-PBS content, phr
PLA/PLA/PLA	0
PLA/PBS/PLA	0
PLA/PBS+PLA-*b*-PBS0.5/PLA	0.5
PLA/PBS+PLA-*b*-PBS1/PLA	1.0
PLA/PBS+PLA-*b*-PBS3/PLA	3.0
PLA/PBS+PLA-*b*-PBS5/PLA	5.0

4.4 Results and Discussion

4.4.1 Structural Characterization of PLA-*b*-PBS Copolymer

PLA and PBS prepolymers were blocked via the Steglich esterification as shown in Scheme 4.1. The successful product was traced with FTIR spectra (Figure 4.1). The characteristic peaks at 1754 cm^{-1} and 1713 cm^{-1} referred to carbonyl group of PLA and PBS prepolymer, respectively are observed. In case of PLA-*b*-PBS copolymer, the split peaks at 1757 cm^{-1} and 1713 cm^{-1} are identified. This indicates that PLA-*b*-PBS copolymer was shown both carbonyl groups of PLA and PBS prepolymers.

Scheme 4.1

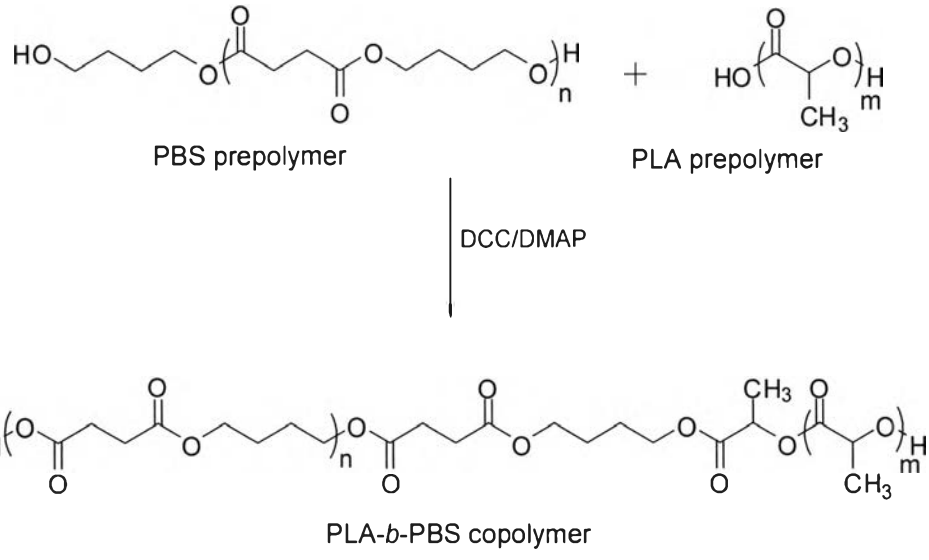

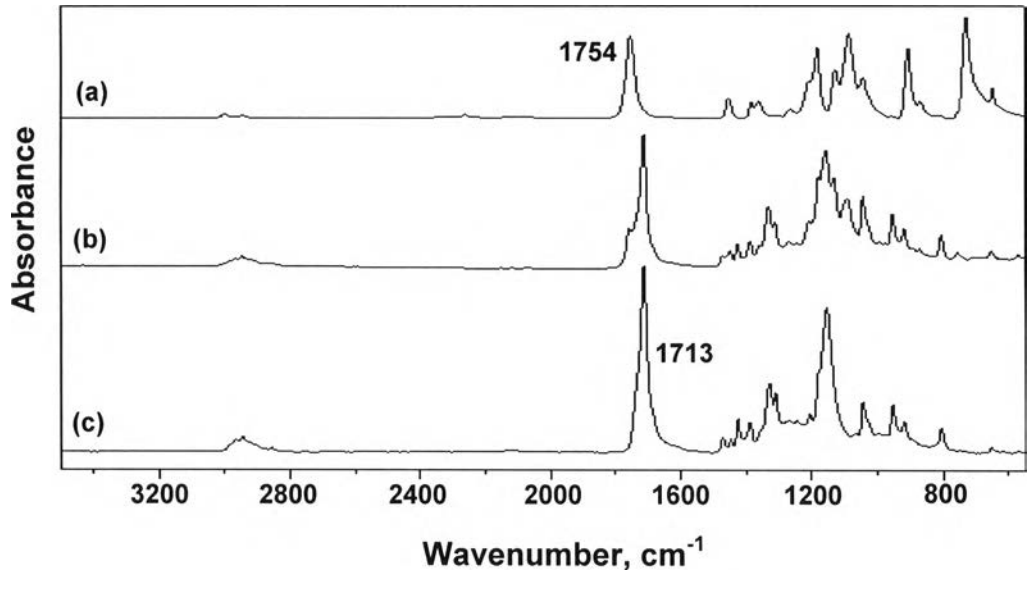

Figure 4.1 FTIR spectra of (a) PLA prepolymer, (b) PLA-*b*-PBS copolymer, and (c) PBS prepolymer.

^{1}H and ^{13}C NMR of PLA-*b*-PBS copolymer was shown in Figure 4.2. In order to clarify the structure of PLA-*b*-PBS copolymer, heteronuclear multiple bond correlation (HMBC) 2D NMR was used. This mode of NMR indicates the correlation between the carbon and proton via multiple bonds. The result shows one

correlation between PLA and PBS units as indicated in the structure in Figure 4.3. The correlation was found between methyl group of PLA unit (at 1.57, 16.75 ppm) and methylene group of PBS unit (at 1.69, 25.34 ppm).

In addition, the number-average molecular weight ($M_{n\text{-}NMR}$) of PLA-*b*-PBS copolymer (3904 g/mole) was calculated according to equation 2 by using quantitative ^{1}H-NMR analysis.[10]

$$M_{n\text{-}NMR} = \left(\frac{I_{1.57}/3}{I_{3.67}/2} \times 72\right) + \left(\frac{I_{2.61}/4}{I_{3.67}/2} \times 172\right) \quad (2)$$

where $I_{1.57}$ is the integral value of the peak at δ_H = 1.57 (3H, d, -O-CH(C**H**$_3$)-) in PLA. $I_{2.61}$ and $I_{3.67}$ are the integral value of the peaks at δ_H = 2.61 (4H, s, -(C=O)-C**H**$_2$-) and 3.67 (2H, s, HO-C**H**$_2$-CH$_2$-) in PBS. 72 and 172 are the molecular weight (g/mole) of PLA and PBS unit, respectively.

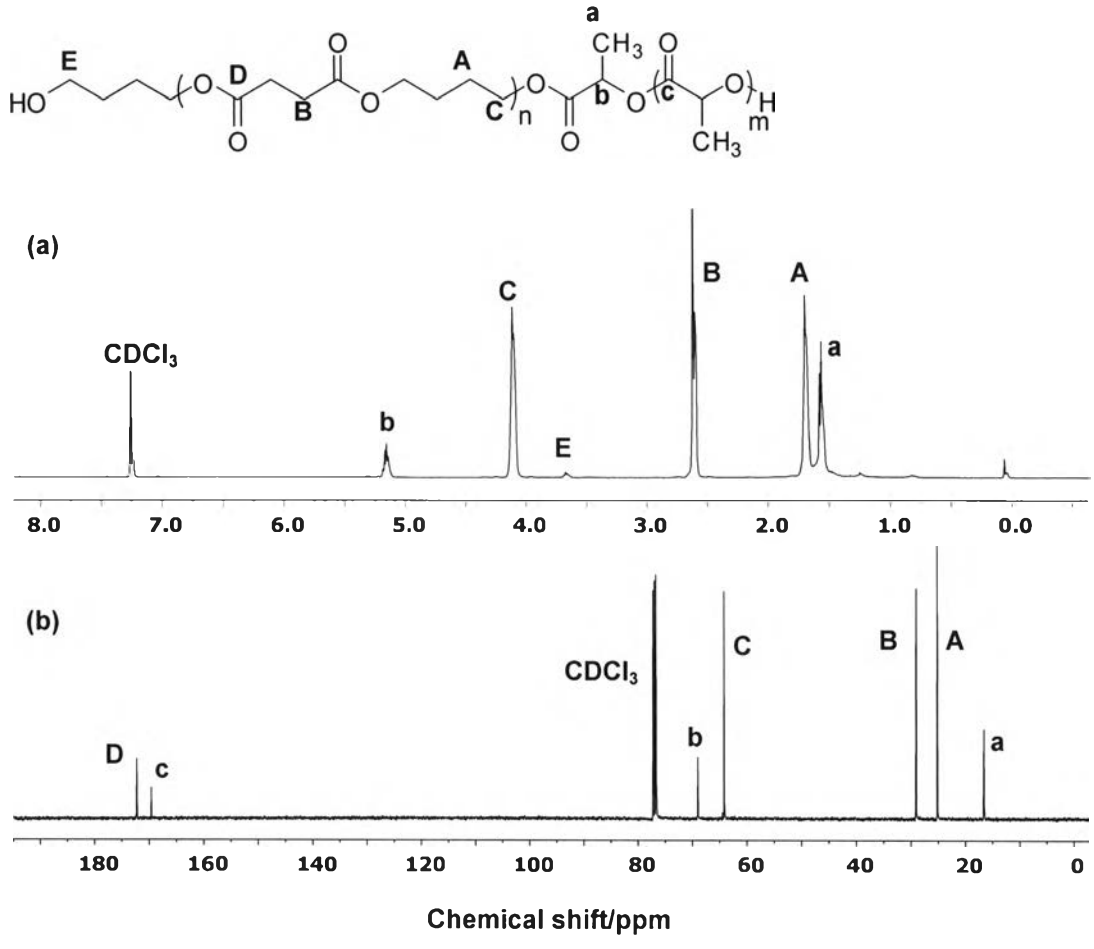

Figure 4.2 (a) ^{1}H and (b) ^{13}C NMR of PLA-*b*-PBS copolymer.

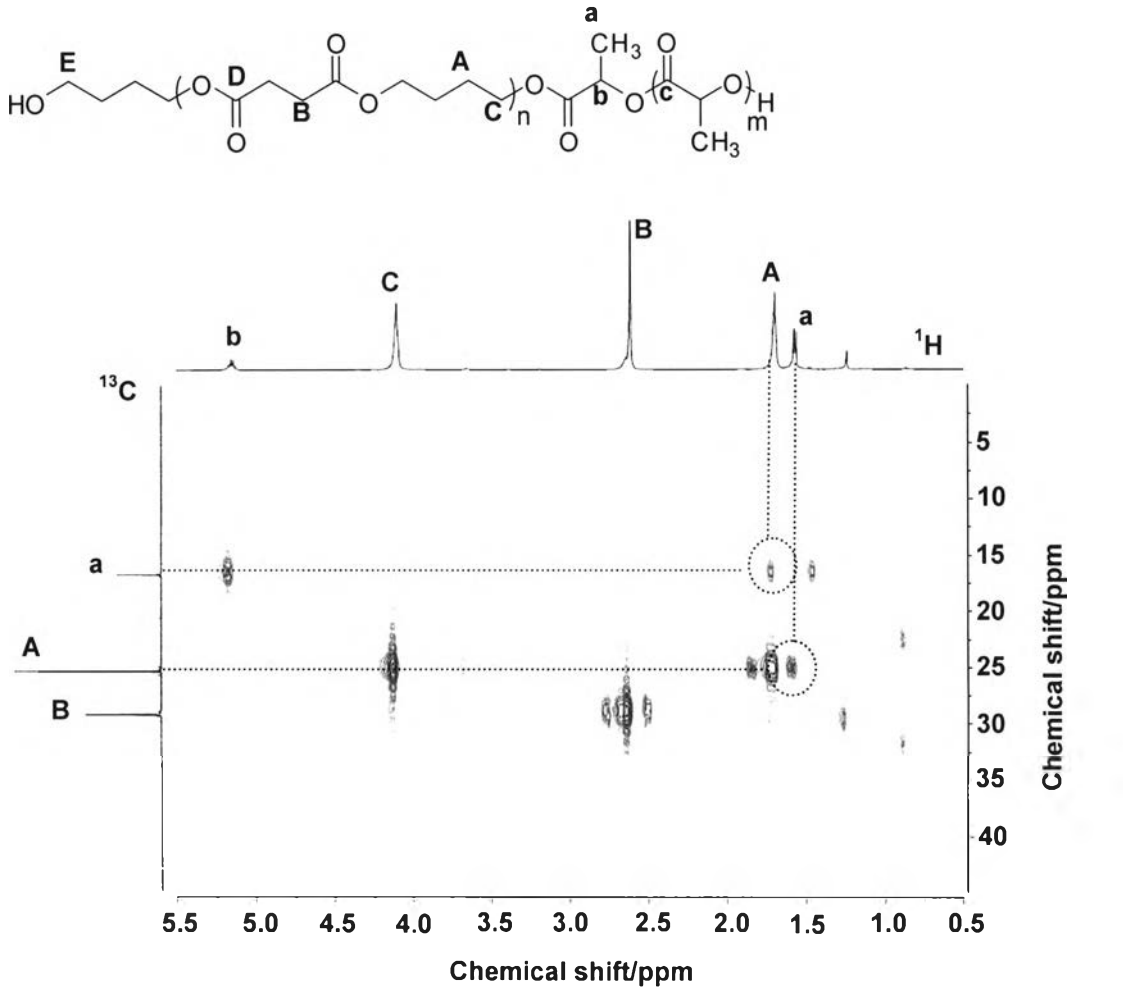

Figure 4.3 ^{1}H-^{13}C HMBC 2D NMR spectrum of PLA-*b*-PBS copolymer.

4.4.2 Characterization of PLA/PBS/PLA Multi-layered Films

4.4.2.1 Compatibility Study

The efficiency of PLA-*b*-PBS copolymer can evaluate from the compatibility of PLA/PBS/PLA multi-layered films containing PLA-*b*-PBS copolymer as a compatibilizer. Figure 4.4((A), (B), (C), (D), (E)) represents morphology of the multi-layered film with 0, 0.5, 1, 3, 5 phr of copolymer, respectively. It is clear that the addition of copolymer shows the improvement of compatibility between PLA and PBS phases as identified by decreasing of the white line between two-phase polymer. This white line refers to interphase which is the boundary between two-phase polymer. In other words, the PLA-*b*-PBS copolymer can increase interfacial adhesion between PLA and PBS polymers.

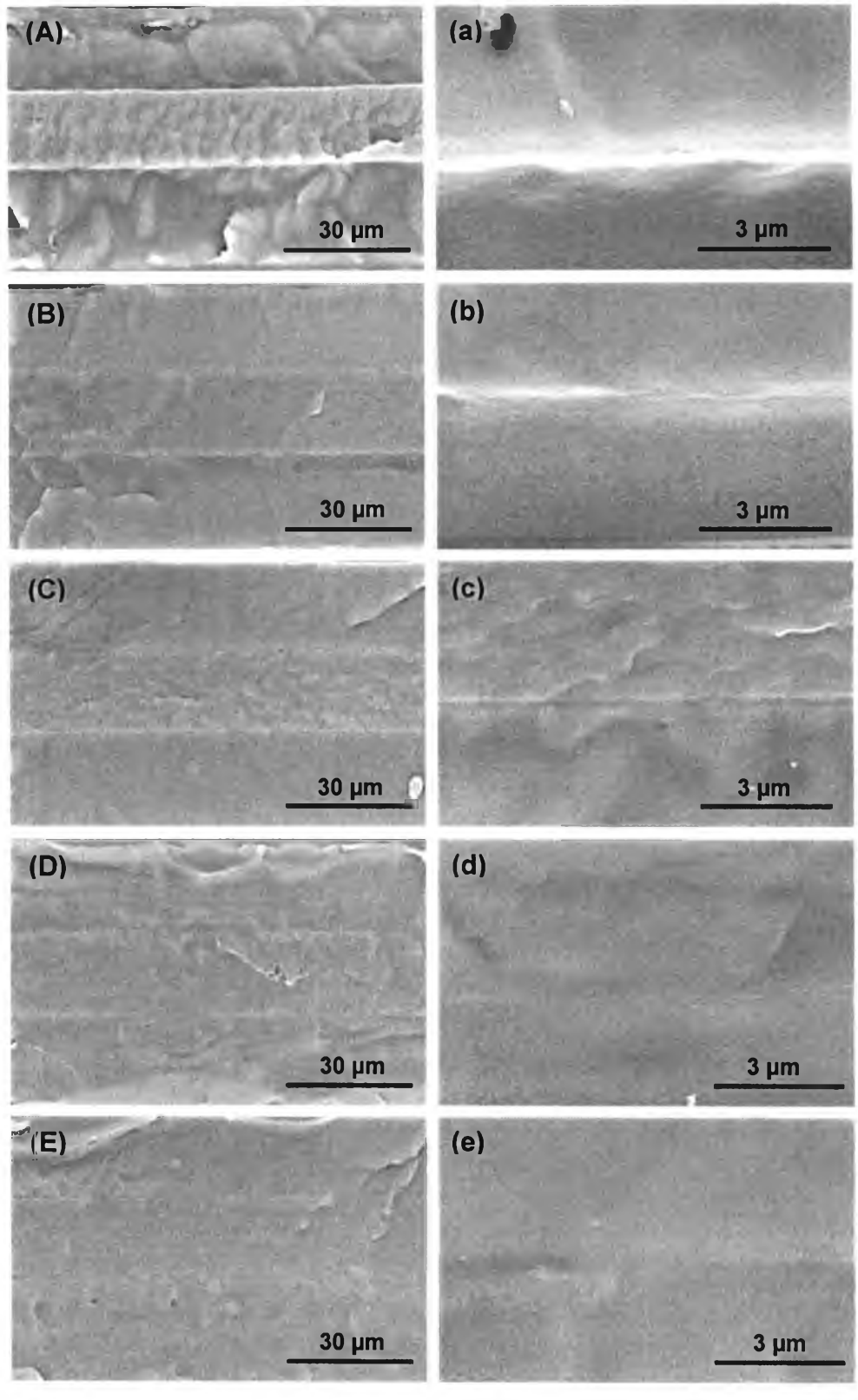

Figure 4.4 SEM images of PLA/PBS/PLA multi-layered films with PLA-*b*-PBS copolymer (A,a) 0 phr, (B,b) 0.5 phr, (C,c) 1.0 phr, (D,d) 3.0 phr, and (E,e) 5.0 phr.

In order to investigate whether PLA-*b*-PBS copolymer interact with PLA and PBS, total correlation spectroscopy (TOCSY) 2D NMR technique was applied. This technique determines the correlation between the proton and proton via multiple bonds. Figure 4.5B represents the PLA/PBS/PLA multi-layered film containing PLA-*b*-PBS copolymer. The correlation at 1.70 ppm (C**H**$_2$-A of PBS) and at 5.17 ppm (C**H**-b of PLA) indicates the interaction of PLA, PBS, and PLA-b-PBS copolymer. It should be noted that the result of PLA/PBS/PLA multi-layered film without PLA-*b*-PBS copolymer was not found any correlation in that region (Figure 4.5A).

GPC technique was also used to confirm the number of component in multi-layered film containing copolymer. It should be mentioned that Figure 4.6c is the mixture of PLA/PBS/PLA multi-layered film and PLA-*b*-PBS copolymer in the solvent of HPLC-grade chloroform ($CHCl_3$), which 2 peaks at 25.762 min (PLA-PBS phases) and 31.876 min (PLA-*b*-PBS) were observed, while Figure 4.6b is the PLA/PBS containing PLA-*b*-PBS/PLA multi-layered film passed extruder. The observation of one peak at 25.807 min in Figure 4.6b implied that PLA-PBS phases and PLA-*b*-PBS copolymer after processing have one component in the system. In other word, some chemical bonds between them were occurred.

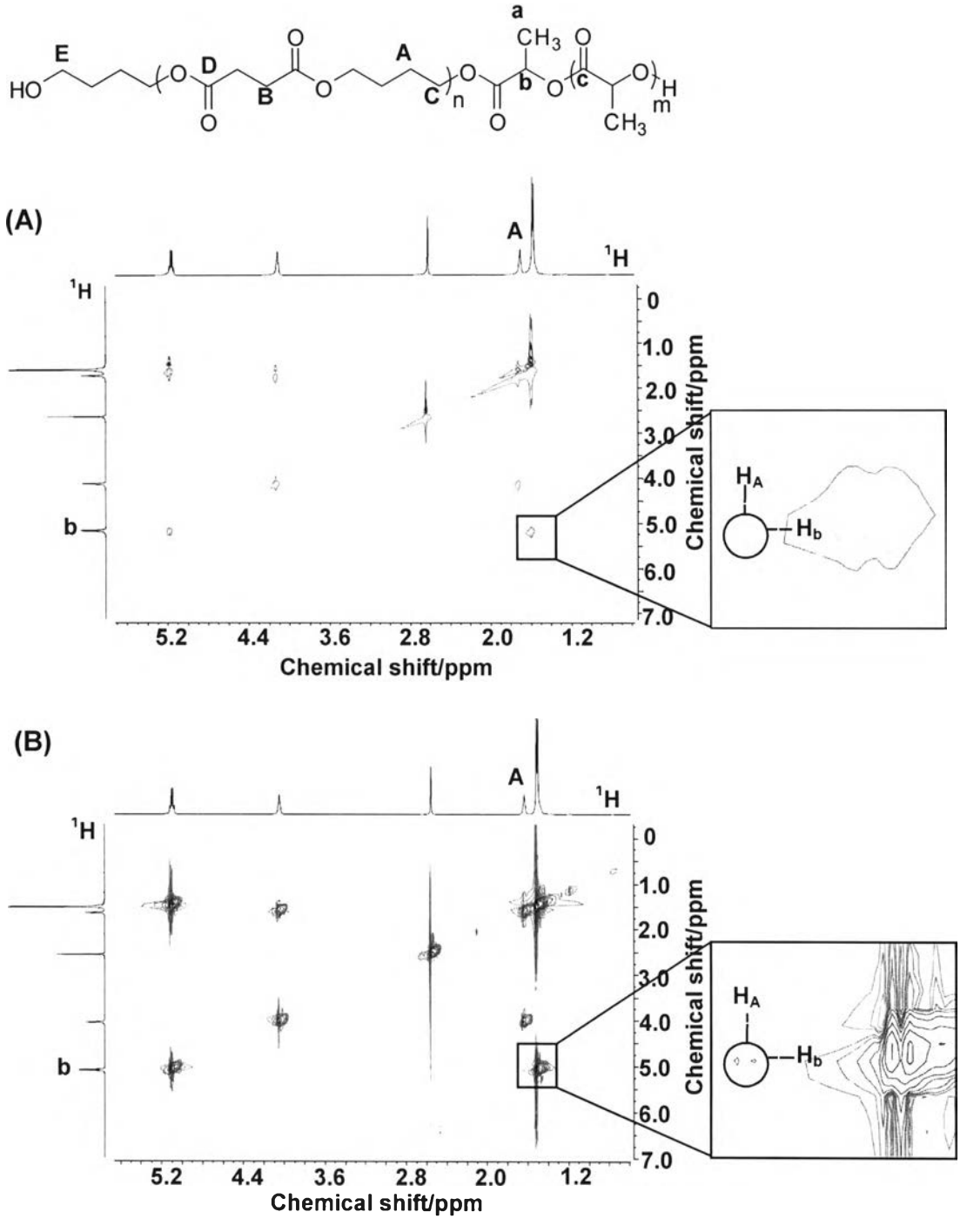

Figure 4.5 ^{1}H-^{1}H TOCSY 2D NMR spectra of (A) PLA/PBS/PLA and (B) PLA/PBS+PLA-*b*-PBS5/PLA multi-layered films.

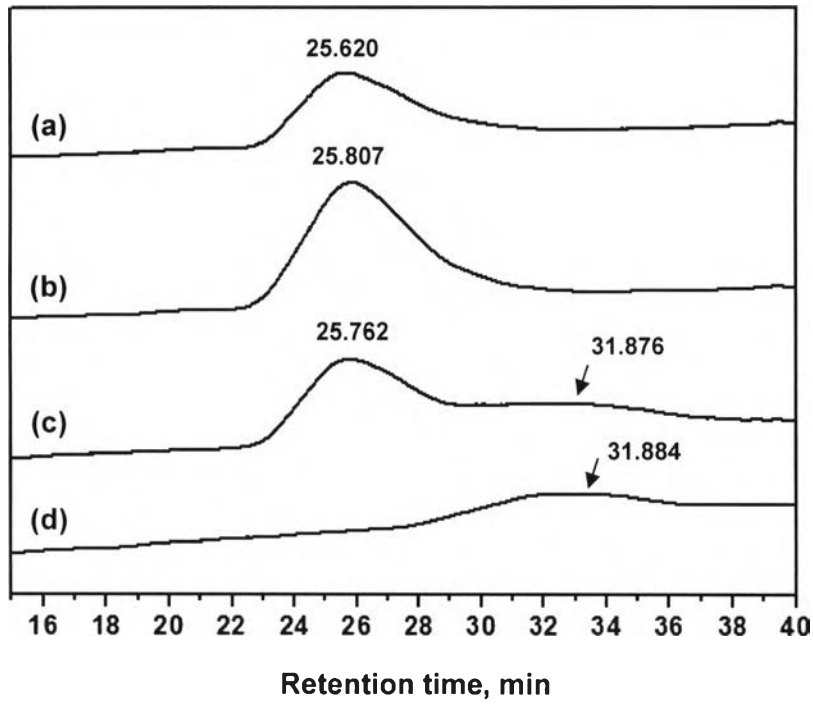

Figure 4.6 GPC chromatogram of (a) PLA/PBS/PLA film, (b) PLA/PBS+PLA-*b*-PBS5/PLA film, (c) PLA/PBS/PLA mixing with PLA-*b*-PBS copolymer 5 phr, and (d) PLA-*b*-PBS copolymer.

4.4.2.2 Mechanical Properties

Figure 4.7 illustrates the mechanical properties of the multi-layered films. The result shows that PLA/PBS/PLA multi-layered film is decreased in tensile strength compared with the PLA/PLA/PLA film. This might be due to the phase separation between the two phases of the different polymers. However, the tensile strength of film is increased when containing PLA-*b*-PBS copolymer for 0.5 phr. In addition, it is clear from this table that the elongation at break is obviously increased for the multi-layered films containing PLA-*b*-PBS copolymer. This might be due to the role of PLA-*b*-PBS copolymer.

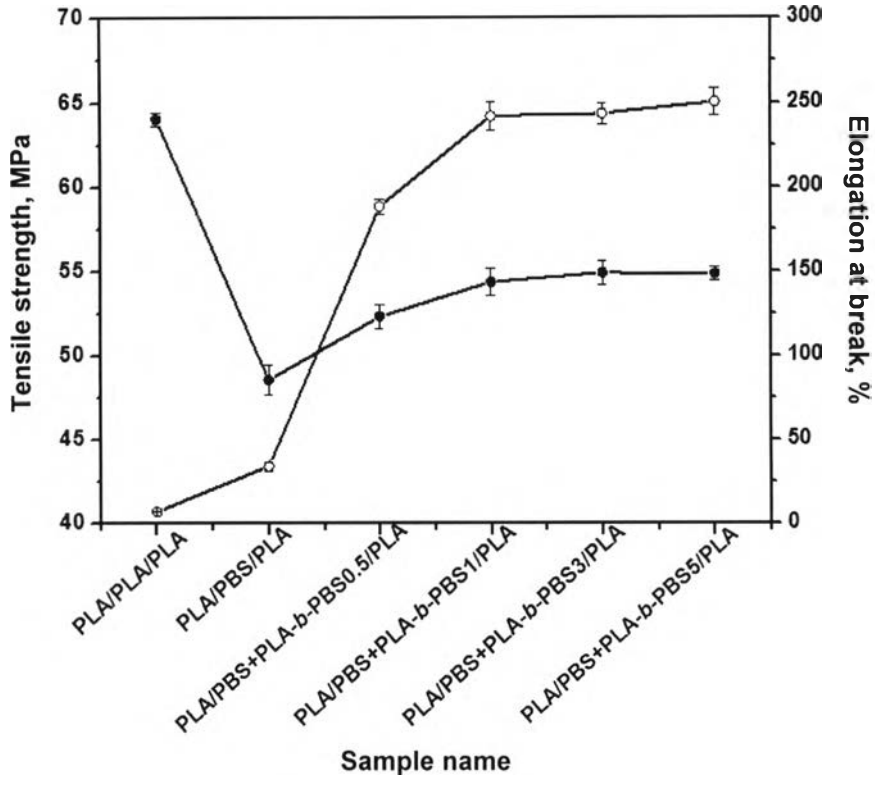

Figure 4.7 Tensile strength and elongation at break of PLA/PBS/PLA multi-layered films containing PLA-*b*-PBS copolymer.

4.4.2.3 Oxygen Permeability

As seen in Figure 4.8, the oxygen permeability of PLA/PLA/ PLA and PBS/PBS/PBS multi-layered films is about 20.0 and 28.5 cm^3 mm m^{-2} day^{-1} atm^{-1}, respectively. Unexpectedly, when PLA and PBS were formed together (PLA/PBS/PLA multi-layered film), the oxygen permeability is decreased (18.4 cm^3 mm m^{-2} day^{-1} atm^{-1}) less than their individual values. This suggests that PLA and PBS are synergistic property in term of oxygen permeability.

The fact that crystallinity can be affected on oxygen permeability.[11] As shown in Table 4.2, PLA/PBS/PLA multi-layered film shows an increase in crystallinity (X_c) from ~0 % to 8.07 % compared with the PLA/PLA/PLA film. It should be noted that this reflects the packing structure of polymer chain resulting in obstructing O_2 molecules. In case of PLA/PBS+PLA-*b*-PBS/PLA multi-layered films, it slightly increases in crystallinity resulting in slightly decrease of oxygen permeability.

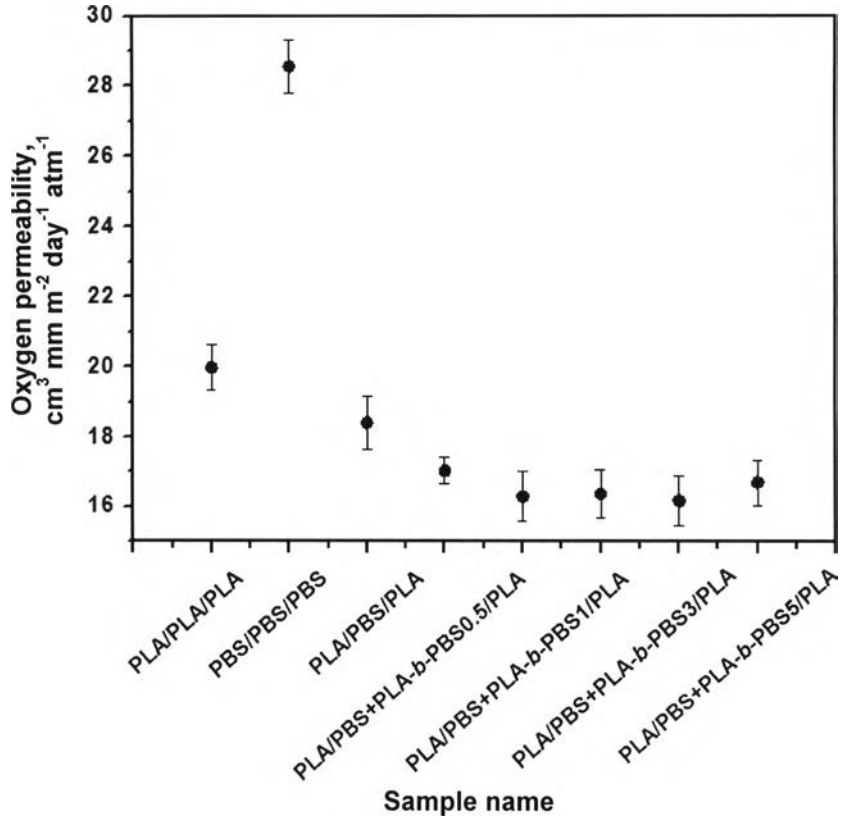

Figure 4.8 Oxygen permeability of PLA/PBS/PLA multi-layered films.

Moreover, XRD analysis was used to characterize the crystallinity pattern of the multi-layered films. The result shows that PBS can induce the crystallization of PLA ($2\Theta = 15.8^{o}$) as seen in Figure 4.9c.

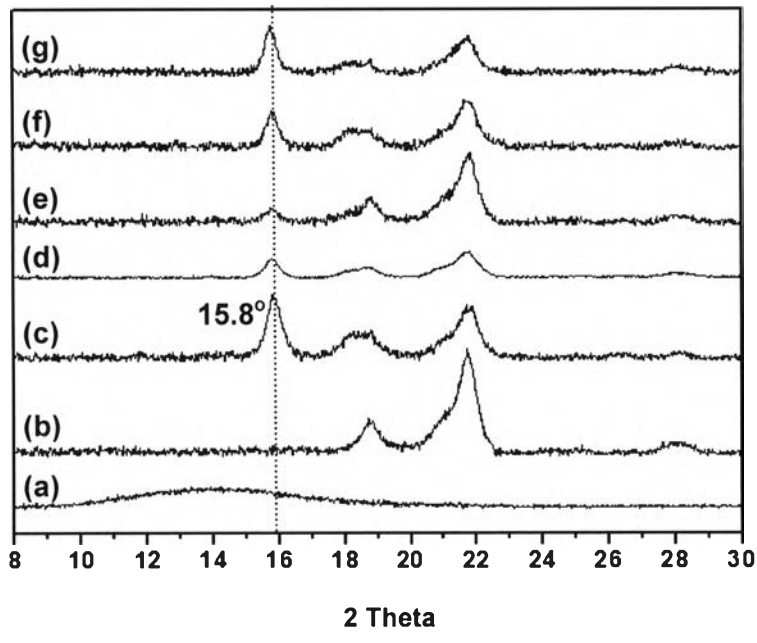

Figure 4.9 XRD pattern of (a) PLA/PLA/PLA, (b) PBS/PBS/PBS, (c) PLA/PBS/PLA, (d) PLA/PBS+PLA-*b*-PBS0.5/PLA, (e) PLA/PBS+PLA-*b*-PBS1/ PLA, (f) PLA/PBS+PLA-*b*-PBS3/PLA, (g) PLA/PBS+PLA-*b*-PBS5/PLA.

4.4.2.4 Thermal Properties and Crystallization Behavior

Thermal propeties and crystallization behavior of the multi-layered films were evaluated using DSC (Table 4.2). The PLA/PBS/PLA and PLA/PBS+PLA-*b*-PBS/PLA multi-layered films show the decrease in T_g with an increase of PLA-*b*-PBS. In other words, the ease of chain mobility occurs when PBS phase contained PLA-*b*-PBS. This leads to an understanding that PLA-*b*-PBS plays the role as compatibilizer for PLA and PBS. The compatibility of PBS and PLA in the multi-layered films also leads to the decrease of T_c as well as the increase of degree of the crystallinity (X_c).

Table 4.2 Thermal properties and crystallinity of PLA/PBS/PLA multi-layered films

Multi-layered film	$T_{g,PLA}$ (°C)	$T_{m,PBS}$ (°C)	$T_{m,PLA}$ (°C)	$T_{c,PLA}$ (°C)	X_c (%)
PLA/PLA/PLA	57.7	-	154.3	101.4	0
PLA/PBS/PLA	55.3	109.0	152.7	85.8	8.07
PLA/PBS+PLA-b-PBS0.5/PLA	54.0	109.2	153.1	85.5	8.52
PLA/PBS+PLA-b-PBS1/PLA	53.5	109.0	152.0	85.1	9.11
PLA/PBS+PLA-b-PBS3/PLA	52.6	108.6	152.6	84.4	10.72
PLA/PBS+PLA-b-PBS5/PLA	52.1	109.1	152.3	84.2	12.01

*All of the data obtained from the first scan.

4.5 Conclusions

The present work demonstrated the PLA/PBS/PLA multi-layered films. By simply copolymerization PLA and PBS with conjugating reaction, PLA-*b*-PBS can be obtained. The addition of PLA-*b*-PBS in PLA/PBS/PLA multi-layered films clarified to us that PLA-*b*-PBS played an important role as compatibility for PLA and PBS. An increased of PLA-*b*-PBS content, in the range of 3-5 phr, led to an increase of film elongation at break for 5-8 times. The compatibility of PLA and PBS also initiated the change in packing structure of PLA as confirmed by the decrease in T_g and T_c as well as the increase in degree of crystallinity. Moreover, oxygen permeability of PLA/PBS/PLA and PLA/PBS+PLA-*b*-PBS/PLA multi-layered films was improved due to the crystallinity factor.

4.6 Acknowledgements

One of the authors (P.S.) would like to acknowledge the Petroleum and Petrochemical College, and Center for Petroleum, Petrochemicals and Advanced Materials, Chulalongkorn University for the M.S. partial scholarship. The

appreciations are extended to Labtech Engineering Co., Ltd. (Thailand) for blown-film process, and the National Research Council for the research fund.

4.7 References

1. **Avérous, L.** (2004) Journal of Macromolecular Science, Part C: Polymer Reviews, **44(3)**, 231-274.
2. **Butler, T.I. and Morris, B.A.** (2009) William Andrew Publishing: Norwich, England, 205-230.
3. **Goulas, A.E., Riganakos, K.A. and Kontominas, M.G.** (2003) Radiation Physics and Chemistry, **68(5)**, 865-872.
4. **Sang II, K. and Deuk-Young, L.** (2012) International Application Published Under The Patent Cooperation Treaty (PCT) WO2012/053820 A2.
5. **Chen, G.-X., Kim, H.-S., Kim, E.-S. and Yoon, J.-S.** (2005) Polymer, **46(25)**, 11829-11836.
6. **Wang, R., Wang, S., Zhang, Y., Wan, C. and Ma, P.** (2009) Polymer Engineering & Science, **49(1)**, 26-33.
7. **Suchao-in, K., Koombhongse, P. and Chirachanchai, S.** (2014) Carbohydrate Polymers, **102**, 95-102.
8. **Mathew, A.P., Oksman, K. and Sain, M.** (2006) Journal of Applied Polymer Science, **101(1)**, 300-310.
9. **Fischer, E. W.; Sterzel, H.; Wegner, G.** ***Kolloid-Z.u.Z.*** *(*1973) Kolloid-Zeitschrift und Zeitschrift für Polymere, **251(11)**, 980-990.
10. **You, Y., Hong, C., Wang, W., Lu, W. and Pan, C.** (2004) Macromolecules, **37(26)**, 9761-9767.
11. **Guinault, A., Sollogoub, C., Domenek, S., Grandmontagne, A. and Ducruet, V.** (2010) International Journal of Material Forming, **3(1)**, 603-606.